Biochimica et Biophysica Acta 1828 (2013) 906–915

Contents lists available at SciVerse ScienceDirect

Biochimica et Biophysica Acta

journal homepage: www.elsevier.com/locate/bbamem

New insights into lipid-Nucleoside Diphosphate Kinase-D interaction mechanism: Protein structural changes and membrane reorganisation

L. Francois-Moutal [a], O. Maniti [a], O. Marcillat [a], T. Granjon [a,*]

[a] Université de Lyon, Université Lyon 1, CNRS, UMR 5246, Institut de Chimie et Biochimie Moléculaires et Supramoléculaires, IMBL, 43 Bd du 11 Novembre 1918 F-69622 Villeurbanne, France

ARTICLE INFO

Article history:
Received 17 May 2012
Received in revised form 18 August 2012
Accepted 28 August 2012
Available online 2 September 2012

Keywords:
NDPK-D
Cardiolipin
Mitochondrion
Fluorescence
Infrared
Brewster angle microscopy

ABSTRACT

Nucleoside Diphosphate Kinases (NDPKs) have long been considered merely as housekeeping enzymes. The discovery of the NME1 gene, an anti-metastatic gene coding for NDPK-A, led the scientific community to re-evaluate their role in the cell. It is now well established that the NDPK family is more complex than what was first thought, and despite the increasing amount of evidence suggesting the multifunctional role of nm23/NDPKs, the specific functions of each family member are still elusive. Among these isoforms, NDPK-D is the only one to present a mitochondria-targeting sequence. It has recently been shown that this protein is able to bind and cross-link with mitochondrial membranes, suggesting that NDPK-D can mediate contact sites and contributes to the mitochondrial intermembrane space structuring. To better understand the influence of NDPK-D on mitochondrial lipid organisation, we analysed its behaviour in different lipid environments. We found that NDPK-D not only interacts with CL or anionic lipids, but is also able to bind in a non negligible manner to zwitterionic PC. NDPK-D alters membrane organisation in terms of fluidity, hydration and lipid clustering, effects which depend on lipid structure. Changes in the protein structure after lipid binding were evidenced, both by fluorescence and infrared spectroscopy, regardless of membrane composition. Taking into account all these elements, a putative mechanism of interaction between NDPK-D and zwitterionic or anionic lipids was proposed.

1. Introduction

The NME gene was initially identified by screening for genes associated with non-metastatic phenotypes [1]. The gene product was later identified as a nucleoside diphosphate kinase (NDPK) [2]. The major role of NDPK isoenzymes is to maintain the pool of different nucleotides within the cell by catalysing the reversible transfer of the terminal phosphoryl group from a nucleoside triphosphate to a nucleoside diphosphate [3]. The neo-synthetized triphosphates are then used for cell anabolic processes, thus making NDPKs one of the main actors in the synthesis of macromolecules. The demonstration of the implication of nm23-H1 in physiopathological processes such as metastasis [4,5] has raised interest in this family of proteins which was then no longer regarded as an 'ordinary' housekeeping enzyme [6]. In humans, ten genes have been reported to code for ten protein isoforms ranging from NDPK-A to D (group I), nm23-H5 to nm23-H9 (Txl2), and XRP2 (group II) [5]. X-ray crystallography indicates that all the enzymes from group I show a homohexamerical structure which possesses a second order symmetry [7–9].

Among these isoforms, NDPK-D is the only one to present a mitochondria-targeting sequence. NDPK-D is ubiquitously expressed, with highest expression levels in the liver, kidneys, bladder and prostate [10]. This kinase binds to the outer face of the inner mitochondrial membrane and was suggested to be associated with mitochondrial contact sites [8,11–13]. Using site-directed mutagenesis and surface plasmon resonance, the groups of Lacombe and Schlattner showed that NDPK-D is able to bind CL-containing liposomes through interaction between a cationic motif (Arg89-Arg90-Lys91) located at the surface of the hexamer and negative charges of the CL polar head group [12]. Moreover, NDPK-D is capable of cross-linking liposomes (since lipid-binding residues are located on symmetric faces of its homohexameric structure), and promotes the transfer of fluorescent lipid probes between liposomes [13]. These characteristics suggest that NDPK-D can mediate contact sites in mitochondria [8] and actively take part in the structuring of the mitochondrial intermembrane space.

To better understand the influence of this protein on mitochondrial lipid organisation, we analysed NDPK-D behaviour in different lipid environments. Intriguingly, we found that NDPK-D not only interacts with CL or anionic lipids, but is also able to bind in a non-negligible manner to zwitterionic PC. A hydrophobic component was also evidenced in the interaction. The effect of NDPK-D on membrane organisation was further investigated in terms of fluidity, hydration or lipid clustering and was found to profoundly depend on lipid structure. Conformational changes in the protein after lipid binding

* Corresponding author at: Université Claude Bernard Lyon 1, Institut de Chimie et Biochimie Moléculaires et Supramoléculaires, CNRS UMR 5246 ICBMS, 43 Bd du 11 Novembre 1918, 69622 Villeurbanne cedex, France. Tel.: +33 472448248; fax: +33 472431557.
E-mail address: thierry.granjon@univ-lyon1.fr (T. Granjon).

0005-2736/$ – see front matter © 2012 Elsevier B.V. All rights reserved.
http://dx.doi.org/10.1016/j.bbamem.2012.08.023

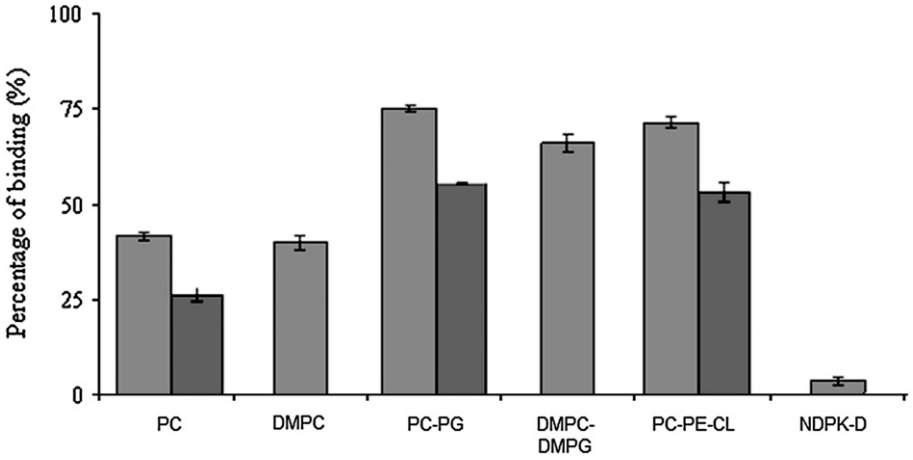

Fig. 1. Percentage of binding of NDPK-D to different liposomes. Binding assays were carried out in the presence (dark grey) or not (light grey) of 150 mM NaCl, with 150 μg of phospholipids and 14 μg of NDPK-D in 200 μL of 20 mM Tris–HCl, pH 7.4, and the percentage of binding was determined from activity measurements in supernatants and pellets after centrifugation. Each column represents the mean ± S.E.M. (bars) of at least three measurements.

occurred, regardless of the membrane composition model. Finally, we propose a putative mechanism of interaction between NDPK-D and zwitterionic or anionic lipids.

2. Materials and methods

2.1. Materials

Phosphatidylcholine (PC) and phosphatidylethanolamine (PE) both extracted from egg yolk were from Lipid Products Acyl chain composition is 32% of 16:0, 2% of 16:1, 11.5% of 18:0, 36% of 18:1, 12.5% of 18:2, and 6% of 20:4 for PC and 22% of 16:0, 37% of 18:0, 30% of 18:1, and 11% of 18:2 for PE (data from Lipid Products). Cardiolipin from bovine heart (CL), phosphatidylglycerol from egg yolk (PG), lactate deshydrogenase and pyruvate kinase were from Sigma.

Dimyristoylphosphatidylglycerol (DMPG), dimyristoylphosphatidylcholine (DMPC) and Laurdan were purchased from Fluka. Ultra pure water was obtained using a Millipore system.

2.2. Bacterial expression and purification of human His-NDPK-D

His-tagged NDPK-D was expressed in *Escherichia coli*, as described in [8], using a pET 28a(+) vector. Recombinant NDPK-D was purified using a modification of an earlier protocol [8]. Briefly, cells were resuspended in 20 mM NaH_2PO_4, pH 7.4, sonicated and centrifuged at 20400 *g* for 30 min at 4 °C. The supernatant was loaded on a Ni-NTA column (Qiagen). NDPK-D was eluted with an imidazole gradient and dialysed against 20 mM Tris–HCl, pH 7.4, 0.1 mM EDTA, 0.2 mM DTT. Protein concentration (0.1 g/L) was determined by the Lowry method using bovine serum albumin as a standard. The purity of the protein was checked with SDS-PAGE.

2.3. Assay of NDPK activity

NDPK activity was measured using a coupled lactate deshydrogenase/pyruvate kinase assay [14]. Decrease of the absorbance at 340 nm was measured. The assays were carried out at 25 °C in 1 mL of reaction mixture containing 50 mM Tris–HCl, pH 7.4, 75 mM KCl, 5 mM $MgCl_2$, 1 mM ATP, 0.1 mM NADH, 1 mM phosphoenolpyruvate, 1 mM TDP and 5U of pyruvate kinase and lactate deshydrogenase.

2.4. Preparation of liposomes

Liposomes were prepared by hydration and extrusion as previously described [15]. Briefly, chloroform solutions of the required lipids were mixed to reach the desired molar ratio, i.e.: PC–PE–CL (2:1:1), PC (100%), DMPC (100%), PC–PG (3:2) and DMPC–DMPG (3:2). Dried lipids were then hydrated (20 mg/mL) in 20 mM Tris–HCl, pH 7.4, 0.1 mM EDTA buffer and dispersed to produce MLV. The lipid suspension was then subjected to 6 freeze/thaw cycles and finally extruded 19 times through a polycarbonate membrane (Avanti Polar Lipids, Alabaster, AL) with 0.4 and 0.2 μm-diameter pores using a mini-extruder [16]. During liposome preparation, lipids were kept at temperatures higher than their gel to liquid crystal transition temperature.

2.5. Interaction of proteins with liposomes

Whatever the phospholipid composition of liposomes, 10 μg of NDPK-D was incubated at 25 °C during 20 min with 150 μg of liposomes. The mixture was then centrifuged at 160000 *g* during 1 h with a Beckman Airfuge. The supernatant was separated from the pellet and the latter was resuspended in 20 mM Tris–HCl pH 7.4, 0.1 mM EDTA solution. We determined NDPK activity in the presence or in the absence of liposomes, whatever the phospholipid composition. As it does not differ, the percentage of binding was determined using the ratio of NDPK activity in the pellet over the total activity (pellet + supernatant).

2.6. Fluorescence measurements

Fluorescence measurements were performed with a Hitachi F4500 fluorometer (150 W Xe). The excitation and emission band-pass values were fixed at 5 nm. Spectra were recorded on the resuspended pellets using a 1 cm path length thermostated quartz cell. All fluorescence spectra were corrected for the baseline spectra of the buffer solution to remove the contribution of the Raman band.

To characterise phospholipid phase coexistence and vesicle physical state fluctuation upon protein binding, Laurdan, a fluorescent probe for which the excitation and emission spectra are sensitive to the environment, was added to the liposomes. Laurdan-specific fluorescence properties allowed us to calculate the generalised polarisation parameter (GP) which was used to determine the effect of NDPK-D on membrane fluidity. The excitation GP was calculated as follows:

$$GP_{exc} = \left(I_g - I_l\right) / \left(I_g + I_l\right).$$

Where I_g and I_l are the fluorescence intensities at the maximum emission wavelength in the gel (440 nm) and in the liquid crystalline (490 nm) phases at a fixed excitation wavelength (360 nm) [17].

Experiments with Laurdan were conducted as follows: phospholipids and Laurdan in a chloroform solution were mixed in a 400:1 molar ratio, and the liposomes were then prepared as previously described. Emission spectra were recorded between 420 and 550 nm, at a fixed excitation wavelength of 360 nm at 37 °C, on 150 μg Laurdan-liposomes in the presence of 14 μg of NDPK-D in a final volume of 150 μL. The phospholipid to protein molar ratio was 29000.

2.7. Monomolecular film formation at the air buffer interface and surface pressure measurements

A circular Teflon trough was filled with 30 mL of 20 mM Tris–HCl buffer, pH 7.4. Monolayers were formed on a clean air-buffer interface by spreading the phospholipids dissolved in chloroform–methanol (4:1) to attain a lateral surface pressure of about 30 mN/m. After pressure stabilisation, a final concentration of 4 nM of NDPK-D was injected in the subphase.

2.8. Brewster angle microscopy

The morphology of lipid and mixed lipid/NDPK-D monolayers at the air/water interface was observed using a Brewster angle microscope (NFT, Göttingen, Germany) mounted on an R&K Langmuir trough (Riegler and Kirstein GmbH, Wiesbaden, Germany). The Langmuir trough and the Brewster angle microscope being in a closed environment, no significant evaporation of the subphase was observed during the experiments. The microscope was equipped with a frequency doubled Nd:Yag laser (532 nm, i.e., 50 mW primary output), a polarizer, an analyzer, and a CCD camera. The spatial resolution of the BAM was about 2 μm and the image size was 430×540 μm. Camera calibration was necessary to determine the relationship between the measured intensity parameter, the grey level (GL), and the reflectance (R). This permitted us to calculate the reflectance as follows: $R = (GL - BG) \times F$ where GL is the recorded grey level value, BG is the background value of the camera and F is the calibration factor for each shutter speed. For ultra thin films, the reflectance depends on both the thickness and refractive index of the monolayer: $R \sim \lambda d^2 n^2$ where λ is the laser wavelength, d the film thickness and n the refractive index of the interfacial film. Consequently, one can use the measured reflectance to estimate the average, or local, thickness of the film.

The monolayer being in a fluid state, a refractive index of 1.46 was used [18,19]. For the mixed protein–lipid monolayer the refractive index is considered to be close to that of the pure lipid because the density of lipids at the interface was relatively high and the refractive index of proteins generally varies over a relatively small range [20].

2.9. Infrared spectra

Liposomes (PC or PC–PE–CL 2:1:1) were prepared as described above, using 20 mM Tris–HCl–deuterium oxide (^2H_2O) (p^{2}H 7.4) buffer. The p^{2}H was measured with a glass electrode and was corrected by a value of 0.4 according to Glasoe and Long [21].

For the assay with protein, the liposome suspension was mixed with 14 μg of enzyme in 20 mM Tris–HCl buffer, pH 7.4, and then incubated 20 min. Separation of liposome-bound and unbound protein was performed by centrifugation at 160000 ×g for 40 min (Beckman Airfuge). The pellet was resuspended in 8 μL of 20 mM Tris–HCl–^2H_2O (p^{2}H 7.4).

Samples were loaded between two BaF_2 circular cells, with a 56 μm Teflon spacer. Fourier Transformed Infrared (FTIR) spectra were recorded with a Nicolet iS10 FTIR spectrometer which was continuously purged with dry air; then 256 scans were collected and co-added per sample spectrum, and Fourier-transformed for each sample. Each FTIR spectrum was representative of at least three independent measurements. The infrared spectra of buffer and residual water vapour were substracted from the infrared spectrum of the sample. Spectra were deconvoluted using PeakFit (Scientific Solutions, Switzerland).

3. Results

3.1. NDPK-D binds to both anionic and zwitterionic membranes

Our first aim was to compare NDPK-D binding to lipids of different polar head and acyl chain compositions. As described in Materials and methods section, liposome-bound NDPK-D was separated from the free protein by centrifugation and NDPK activity was measured in each fraction. The percentage of NDPK-D activity recovered in the LUV-bound fraction is shown in Fig. 1. Binding of NDPK-D to PC–PE–CL or PC–PG membranes was 75% in our conditions (phospholipids to protein molar ratio of 29000). In the same conditions, but in the absence of liposomes, less than 5% sedimentation of NDPK-D was observed. We considered that this percentage is negligible compared with those obtained in the presence of liposomes. Whatever the nature of the negatively charged phospholipid, PG or CL, the binding percentage remained unchanged (75% for PC–PG (3:2) against 73% for PC–PE–CL (2:1:1)), thus, NDPK-D interaction seems to be independent of the nature of the anionic polar head. The percentage of binding to saturated and unsaturated phospholipids was similar (about 70% for DMPC:DMPG and 75% for PC:PG), which indicated that the saturation of the acyl chains of the phospholipids had no major influence on the NDPK-D binding.

Interestingly, in the presence of a zwitterionic membrane (PC), the percentage of bound NDPK-D was about 45%. Thus, although binding of NDPK-D activity was higher with anionic phospholipids, a non negligible interaction was found with the zwitterionic lipid PC. In order to obtain further information about the nature of the interaction, the same experiment was repeated in the presence of 150 mM NaCl. In these conditions, the percentage of NDPK-D bound to PC liposomes decreased from 45% to 25%, while the percentage of NDPK-D bound to negatively charged liposomes, PG or CL, decreased from 70% to 54%. Increasing NaCl concentration up to 0.3 M did not further reduce the amount of NDPK-D bound to liposomes (not shown). Thus, NDPK-D can bind to all types of vesicles tested even at a non-physiologically high ionic strength.

3.2. Structural changes of NDPK-D after membrane binding

We next used fluorescence and FTIR spectroscopies to determine whether protein conformation was modified upon binding to liposomes with different phospholipid compositions.

First, NDPK-D intrinsic fluorescence emission spectra were recorded in the absence of lipids or after binding to liposomes and removal of the unbound protein. Maximal emission wavelengths were determined with an excitation wavelength of 295 nm and are shown in Table 1.

The 340 nm maximum emission wavelength of the protein in the absence of lipids indicates a rather hydrophilic average environment of the tryptophan side chain. In the presence of liposomes, whatever the phospholipid composition, the maximum was shifted to lower values (335–333 nm). These results suggest that at least one of the tryptophan residues is directly affected by the binding process and/or that NDPK-D binding to membranes changes the environment of these tryptophan residues into a more hydrophobic one. The presence of either 150 or 300 mM NaCl has no effect on this shift.

We also used FTIR spectroscopy to assess the effect of NDPK-D binding to PC–PE–CL or PC liposomes on its structure. The amide I band, which is dominated by carbonyl vibration, reflects the protein's secondary structure and is therefore an important tool for analysing changes in protein conformation. Spectra of the amide I region of free or bound NDPK-D are presented in Fig. 2A and B. Second derivative was used to locate position of the different absorption bands on

Table 1
Maximum emission wavelength of NDPK-D alone or bound to liposomes in the presence or absence of 150 mM NaCl.

NDPK-D	Unbound	PC	DMPC	PC–PG	DMPC–DMPG	PC–PE–CL
λ Max (nm)	340	334	333	335	333	333
λ Max (nm) + NaCl	340	333	334	335	333	334

the spectra (as shown in Fig. 2A and B, grey lines) which were further deconvolunted using Peak-FitTM software (Fig. 2C and D).

As expected from the crystallographic structure, the free NDPK-D IR spectrum (Fig 2A) exhibited a main band around 1660–1650 cm^{-1}, characteristic of proteins with a high proportion of helix structure [8,22,23]. Second derivative spectrum indicated that the amide I region was indeed made of several components, two of which were located in the region of α helix vibration bands, at 1654 cm^{-1} and 1662 cm^{-1}. Another major band located at 1644 cm^{-1} can be attributed to random structures [22]. Several peaks/contributions were also present in the 1630–1612 cm^{-1} and 1670 and 1690 cm^{-1} region. Both band splitting and band position are characteristic of different types of beta sheet structures [22,24].

As shown in Fig. 2B, NDPK-D binding to liposomes modified the amide I region of the protein IR spectrum. The two bands observed in the α helix region were shifted to lower wavenumbers: 1649 cm^{-1} and 1659 cm^{-1}. Moreover, deconvolution of spectra indicated that binding of NDPK-D to liposomes also changed the area of the different bands as shown in Fig. 2D. The high wavenumber (alpha helix contribution) represented only 14% of the spectrum of the protein alone instead of 31% for the bound protein, whereas upon protein binding, the lower wavenumber component was reduced from 24% to 19%. In the β-sheet region, the 1632 cm^{-1} component decreased 3 fold, from 15% to 5%, when NDPK-D bound to the membrane. It should be noted that the 1680 cm^{-1} band increased in the presence of liposomes (3.5% versus 10%). The other bands (1612 cm^{-1}, 1622 cm^{-1}, 1672 cm^{-1} and 1690 cm^{-1}) were only marginally modified by the interaction between NDPK-D and liposomes. The amide I bands on spectra recorded with NDPK-D bound to either PC (not shown) or PC–PE–CL liposomes (Fig. 2B) were identical.

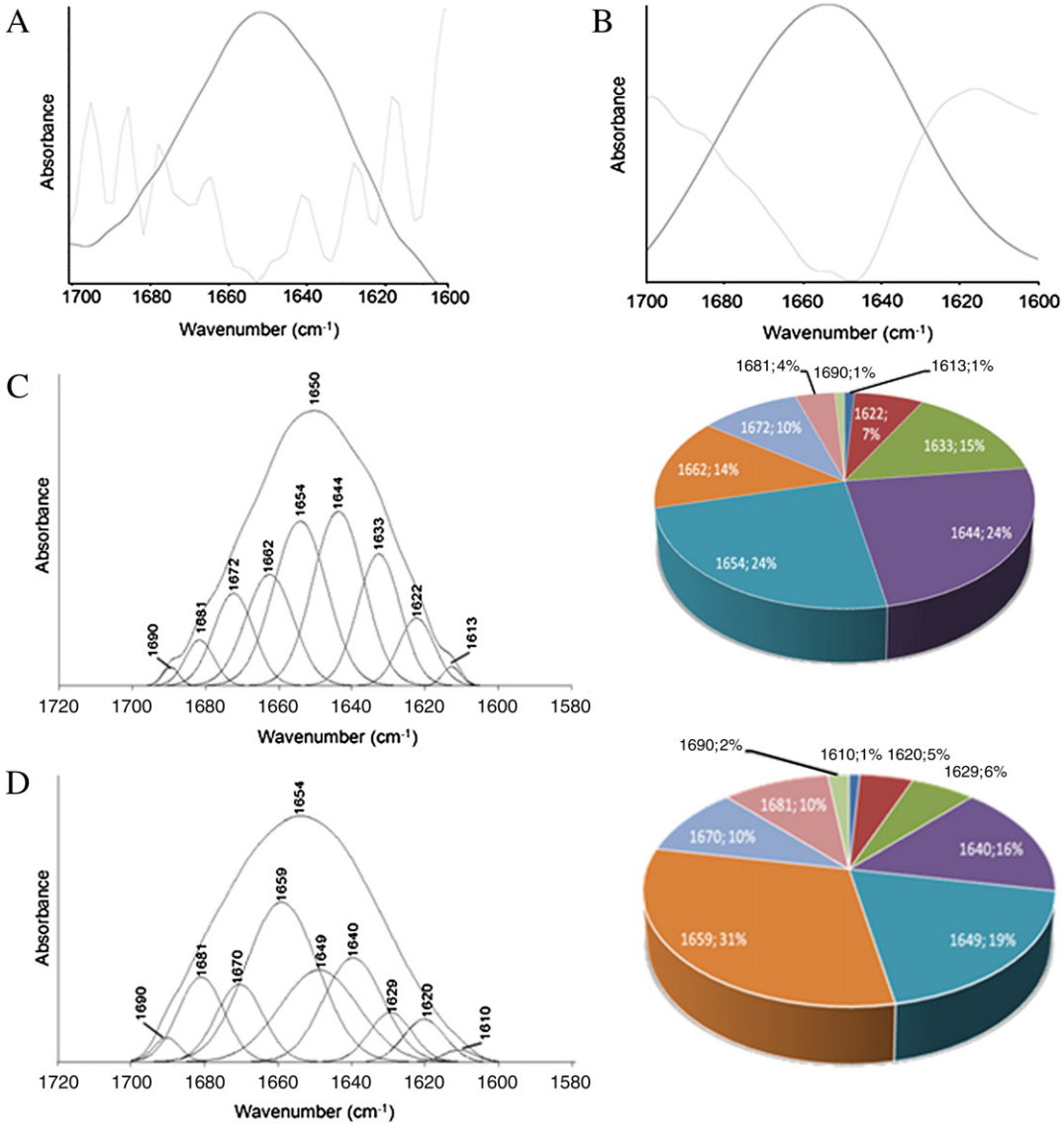

Fig. 2. Infrared spectra (black), in the region of the amide I band, of NDPK-D bound (B) or not to PC–PE–CL (A). In grey is the second derivative. (C) Fitting curves of the different components of the amide I band of the NDPK-D alone, or bound to PC–PE–CL liposomes (D). (E) Percentages of the peak area of each component of the amide I spectra.

3.3. NDPK-D modifies membrane fluidity and organisation

3.3.1. NDPK-D effect on Laurdan fluorescence in liposomes

The fluorescence properties of Laurdan were used to monitor local changes in the immediate vicinity of the probe due to protein binding. Laurdan GP (Generalised Polarisation, see Experimental section) allows one to study variations of the membrane physical state. Liposomes were made of either unsaturated PC–PE–CL (2:1:1) or saturated DMPC–DMPG (3:2) or DMPC. The use of saturated phospholipids allowed us to work at temperatures close to the phase transition temperature of the lipids and thus to enhance the effect of the protein binding on the mobility of solvent molecules surrounding Laurdan. Data were expressed as the variation in GP observed with and without NDPK (delta GP) and showed that NDPK-D binding only marginally modified the GP value of Laurdan inserted in DMPC ($\Delta GP = 0.009$) (Fig 3) or PC liposomes (data not shown). This indicates that NDPK-D did not significantly affect the physical state of vesicles exposing phosphatidylcholine polar heads. However, a significant increase in GP was recorded with vesicles containing anionic phospholipids. Indeed, the binding of the protein to DMPC–DMPG (3:2) vesicles leads to a ΔGP value of 0.087. NDPK-D had a more moderate influence at the liposome membrane level of PC–PE–CL (2:1:1) with an increase in the GP value of 0.030. This indicates a modification of the mobility of water molecules surrounding Laurdan after protein binding.

3.3.2. Protein effect on lipid infrared absorption bands

Alterations in hydrogen bonding, orientation of the head group, and differences in chain packing of phospholipids after NDPK-D binding to the phospholipid bilayer were further monitored at the O – P – O, C═O and CH_2 stretching vibration level using infrared spectroscopy [25,26].

Binding of NDPK-D to liposomes that do or do not contain anionic charges, resulted in a shift of the symmetric PO_2^- stretching band respectively from 1092 to 1070 cm^{-1} for both PC–PE–CL and PC liposomes (Fig 4). This can be interpreted as alterations in head group hydration or increased hydrogen bonding at the polar surface of phospholipids following protein binding [25].

The phospholipid ester bonds (C═O) stretching vibration of the lipid bilayer were also affected by the binding of NDPK-D (Fig 5). In the absence of protein, with both PC and PC–PE–CL liposomes a single broad carbonyl peak centred around 1733 cm^{-1} was observed. This broad carbonyl peak was composed of two separate components, as indicated by second derivative minima (not shown): a "dehydrated" carbonyl (1742 cm^{-1}) and a "hydrated" carbonyl (1727 cm^{-1}) [26]. Addition of NDPK-D (Fig. 5) induced an increase in the 1742 cm^{-1} contribution, without change in the position of the two components. This thus suggests an increase in the content of dehydrated carbonyl bonds.

The location of the C – H stretching vibration is an indicator of the C – H bond motional freedom: the higher the wavenumber, the greater the acyl chain mobility. Minute variations induced by protein binding can thus be evidenced as a shift in this very sensitive vibrational band [27]. The effect of NDPK-D binding on the CH_2 vibration was dependent on phospholipid head group. Indeed, protein binding to zwitterionic liposomes induced no significant changes on phospholipid asymmetric (Fig. 6) and symmetric (not shown) CH_2 stretching bands (2924 and 2853 cm^{-1} respectively). On the contrary, adsorption of NDPK-D on PC–PE–CL vesicles led to a small shift of symmetrical and asymmetrical CH_2 bands from 2853 to 2854 cm^{-1} and from 2924 cm^{-1} to 2925 cm^{-1} respectively.

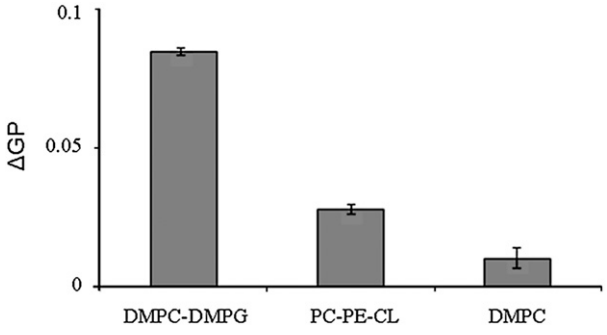

Fig. 3. Variation of Laurdan excitation GP in different liposomes in the presence of NDPK-D. Each column represents the mean ± S.E.M. (bars) of at least three measurements.

3.3.3. Lipid clustering on monolayers after NDPK-D interaction

To see whether NDPK-D was able to perturb the lateral organisation of the membrane, phospholipid monolayers were used as membrane models and changes in the lateral phospholipid organisation were followed by Brewster angle microscopy (BAM). First, a phospholipid mixture of PC–PE–CL in a 2:1:1 molar ratio, mimicking the composition of the inner mitochondrial membrane, was spread at the air/buffer interface at a lateral surface pressure of about 30 mN/m. At

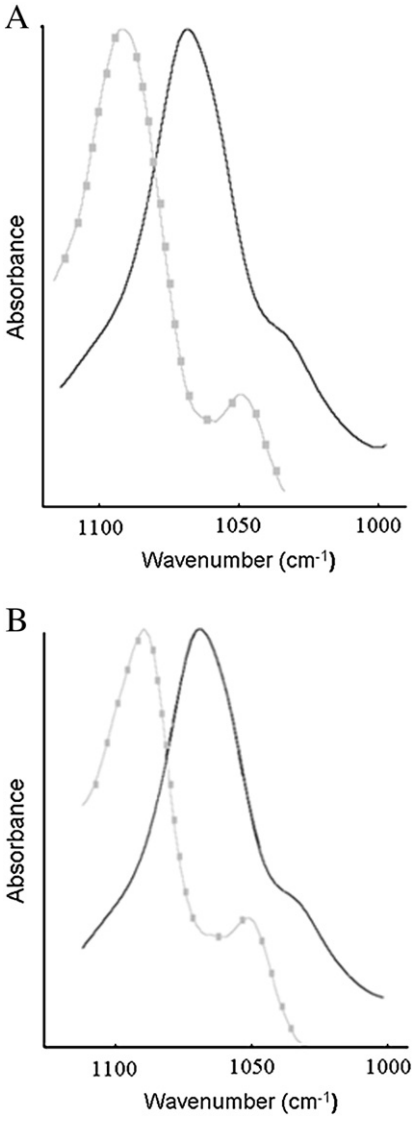

Fig. 4. Infrared spectra in the region of the PO_2^- stretching vibration. 160 μg of PC–PE–CL (A) or pure PC (B) alone (grey) or with (black) 14 μg of NDPK-D. Samples were suspended in 8 μL of 20 mM Tris–HCl–^2H_2O, p^{2}H 7.4, as described in Materials and methods.

this surface pressure it is generally considered that lipids have the same thermodynamic characteristics as in biological membranes [28]. BAM images of the PC–PE–CL mixture showed a homogeneous surface (Fig. 7A). About 10 min after injection of 4 nM NDPK in the buffer phase, bright spots began to appear and increased in number but not in size. The local thickness at these bright spots was estimated at about 6.5 nm (using a refractive index of 1.46, see Experimental section). As a control, the experiment was also done without protein. The general aspect of the lipid monolayer as well as the local thickness of the monolayer (1.6 nm) remained unchanged over the course of the experiment (not shown).

The same experiments have been performed with PC, PE, PC–PE (3:1) and with CL monolayers. With a PC (Fig. 7B), PE or PC–PE monolayers (not shown), BAM images showed a homogeneous surface with no bright domains. Two hours after injection of the NDPK-D underneath the monolayer, BAM images were quite similar to those obtained in the absence of protein.

BAM images of a pure CL monolayer at about 30 mN/m, exhibited a homogeneous surface without any bright domains. However, 30 min after injection, BAM images exhibited bright spots as shown in Fig. 7C. The number of bright spots increased with time, more than in the presence of PC–PE–CL, indicating that the formation of such bright clusters was associated with NDPK-D interactions with CL.

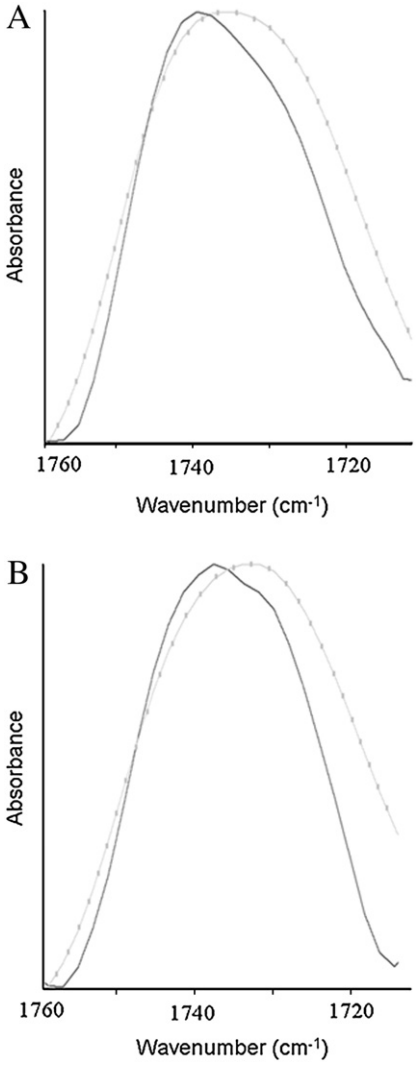

Fig. 5. Infrared spectra in the region of the ester stretching vibration. 160 μg of PC–PE–CL (A) or pure PC (B) alone (grey) or with (black) 14 μg of NDPK-D. Samples were suspended in 8 μL of 20 mM Tris–HCl–^2H_2O, p^{2}H 7.4, as described in Materials and methods.

3.3.4. Structural models of NDPK-D binding to CL, deduced from the BAM pictures

As mentioned above, on a pure CL monolayer no spots were observed before NDPK-D injection, but addition of NDPK-D induced the formation of bright aggregates. Views of the CL monolayer in the presence and absence of NDPK-D were reconstructed. The aspect of the pure CL membrane was homogenous with a maximum thickness of 1.4 nm (Fig. 7D), while in the presence of NDPK-D the interfacial film was irregular with a maximum thickness of 6.5 nm (Fig. 7E).

The film thickness profile was calculated along the white line in image 7F from image 7C. Based on the brightness of the BAM pictures indicating changes in the reflectivity at the interface, the apparent thickness of the interfacial film was modelled at each point of the BAM picture.

4. Discussion

Nucleoside diphosphate kinases (NDPKs) are nucleoside-metabolising enzymes participating in cellular high energy phosphoryl transfer as well as in several apparently unrelated biological processes. Several isoforms of NDPK have been reported, which differ in their specificity and subcellular localization. NDPK-D, the mitochondrial isoform, has been shown to be involved in several physiological processes such as fatty acid metabolism, proteins and nucleic acid synthesis, and is known to interact with Krebs cycle enzymes. Moreover, although the role of NDPK-D in cancer progression is not known, overexpression of this protein has been reported in colorectal and kidney carcinoma [29].

Since NDPK-D is retrieved at the mitochondrial membrane, we analysed its interaction with phospholipids on two complementary systems, liposomes and monolayers.

A first aim of this work was to assess NDPK-D lipid binding partner(s) at the membrane. Intriguingly, we observed that NDPK-D not only interacts with liposomes containing anionic lipids, but also shows a non negligible binding to zwitterionic lipids such as PC. Moreover, this interaction is not abolished in the presence of NaCl, suggesting

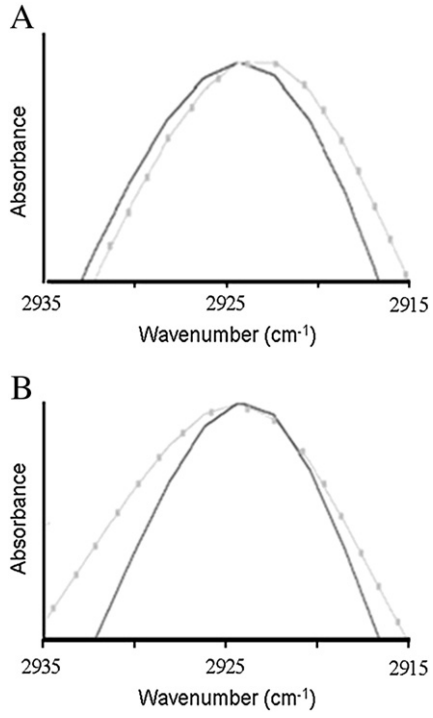

Fig. 6. Infrared spectra in the region of the asymmetric CH stretching vibration. 160 μg of PC–PE–CL (A) or pure PC (B) alone (grey) or with (black) 14 μg of NDPK-D. Samples were suspended in 8 μL of 20 mM Tris–HCl–^2H_2O, p^{2}H 7.4, as described in Materials and methods.

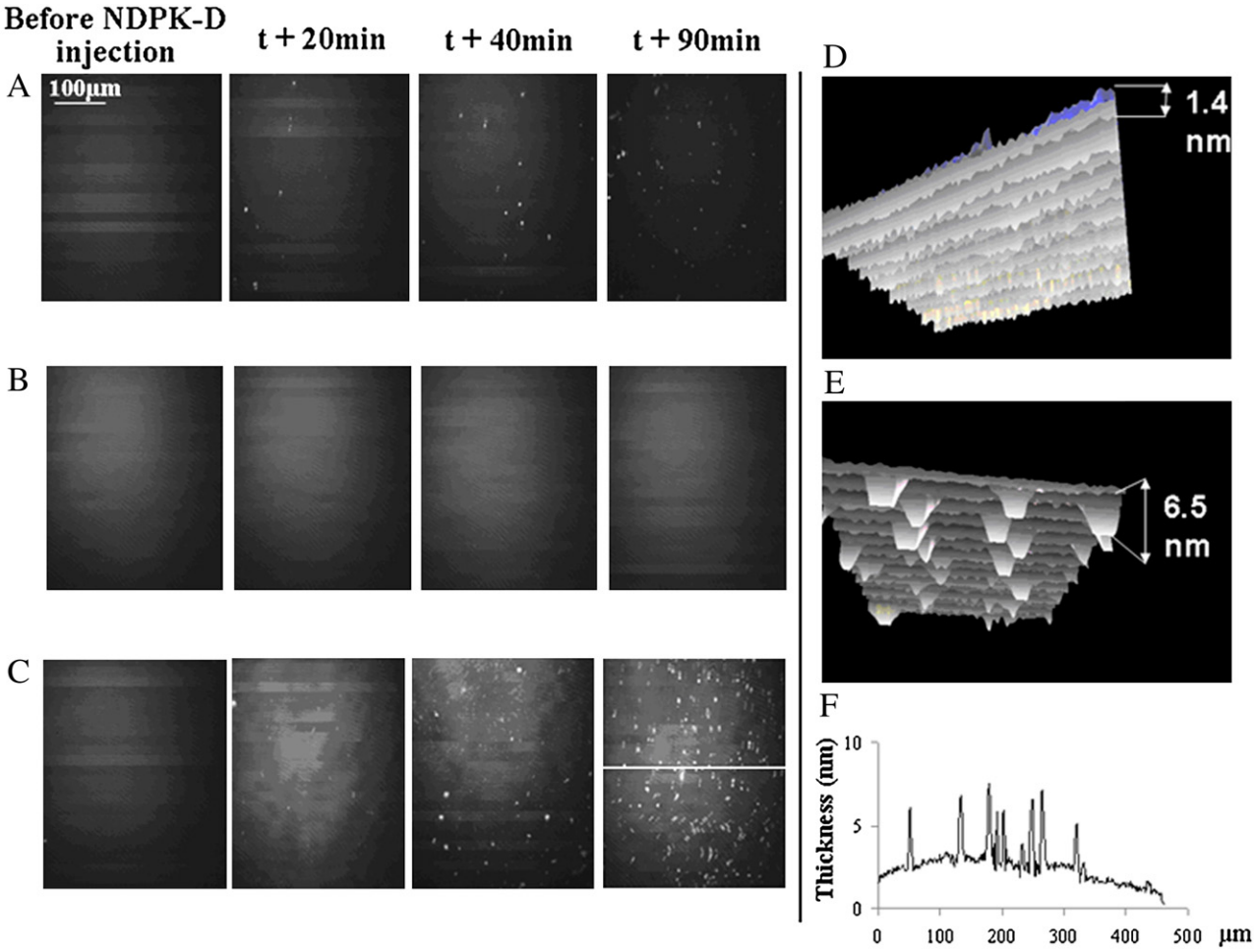

Fig. 7. BAM images of (A) PC–PE–CL, (B) PC and (C) CL monolayers at 30 mN/m, at different incubation times. Shutter speed was 120 s^{-1} for each image. Theoretical 3D simulation of a CL monolayer in the absence (D) or presence (E) of NDPK-D. (F) Film thickness profile along the white line in image C.

that the interaction process is not exclusively electrostatic but also involves a strong hydrophobic component. We decided thus to investigate whether this multi-component interaction process was accompanied by protein structural modifications.

5. Effect of membrane binding on protein structure

In the presence of liposomes, a 5–7 nm blue-shift of NDPK-D tryptophan maximum emission wavelength is observed, indicating that the environment of one or more tryptophan residue's side chain becomes more hydrophobic. It has been shown that NDPK-D binding to membranes involves the sequence Arg89-Arg90-Lys91 which is localised in a hairpin between the αA and α2 helices (Fig. 8) [12]. Among NDPK-D tryptophans, residue 166, which is close to the hairpin (Fig. 8), may be the one most affected by membrane binding. The blue shift could result from a direct interaction of the tryptophan side chain with the lipid bilayer as described for a number of peptides or proteins (human dystrophin [30], LL-37 [31], amphibian antimicrobial peptide DD K [32], and melittin [33]). Alternatively, the spectral shift could be the result of a conformational change of the protein with a tryptophan that would become buried within the structure.

The effect of NDPK-D binding on its secondary structure was then studied by infrared spectroscopy. NDPK-D infrared spectrum in the amide I band region was clearly dominated by α helical contribution as shown in Fig. 2A. Secondary derivative and deconvolution spectra reveal that this contribution is due to two distinct components at 1662 and 1654 cm^{-1}, indicative of the coexistence of two types of

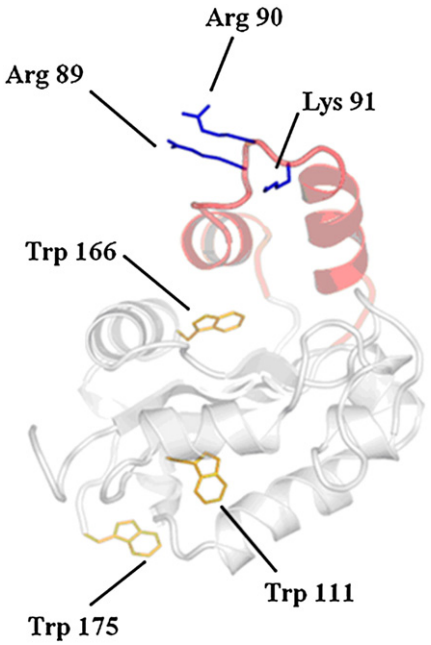

Fig. 8. Monomer of NDPK-D: (PDB: 1ehw) visualised with Accelrys ViewerLite5.0. The flexible region is coloured in red, the binding triad in blue and the tryptophans in yellow.

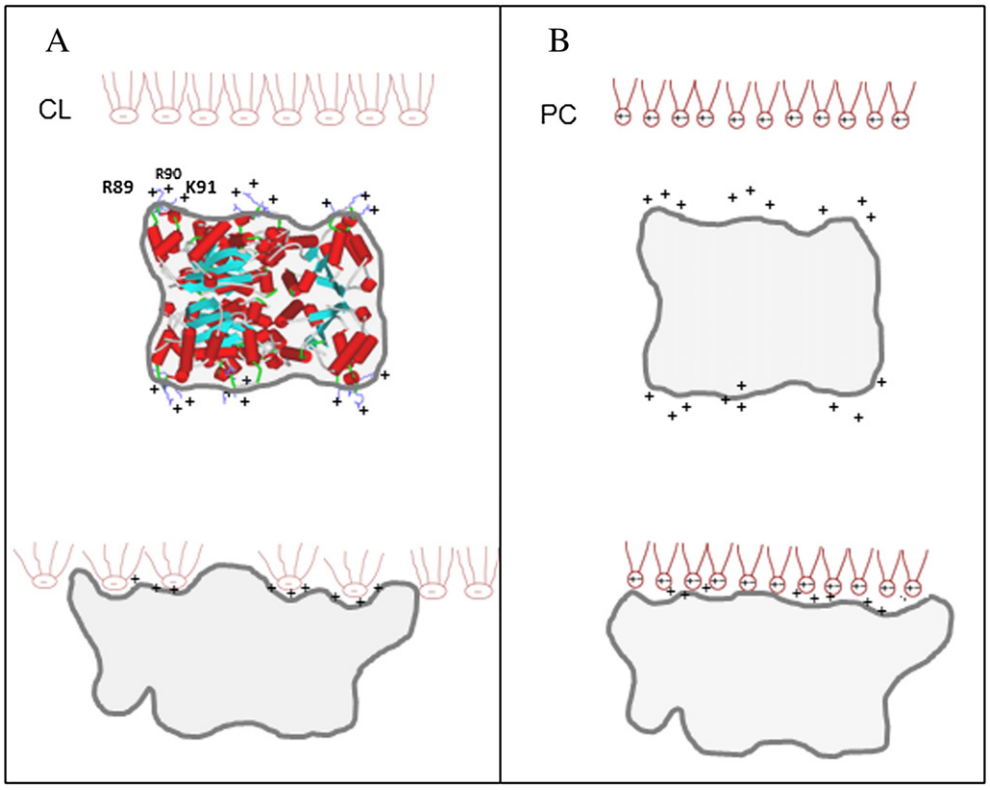

Fig. 9. Cartoon model of NDPK-D interaction with CL (A) or with PC membranes (B). Only the outer leaflet of the bilayer was represented. After binding to lipids, NDPK-D undergoes conformational changes and inserts part of the molecule between lipid head groups. Insertion leads to water molecule removal and moves lipid molecules apart. This effect is more pronounced with CL membranes and allows a higher mobility at the acyl chain level.

α helical structures. This is reminiscent of what has been shown for the secretory phospholipase A2 once bound to lipid bilayers [34], bacteriorhodopsin [35] and oxaloacetate decarboxylase [36]. Since the position of vibrational bands depends on hydrogen bonding [24], the band at 1662 cm^{-1} is thus likely to correspond to more flexible and more dynamic α helices than the 1654 cm^{-1} one. The region of β-sheet vibrational bands also presented several distinct contributions at 1622, 1633, 1672 and 1682 cm^{-1} considered as a mixture of antiparallel β sheets, β turns and open loops [22].

Binding of NDPK-D on PC–PE–CL liposomes induced a modification of the amide I spectra. Overall, the protein–lipid interaction shifted the different contributions to lower wavenumbers, suggesting that lipid binding altered hydrogen bonding. The proportions of the main secondary structures were also modified. On the one hand, the presence of lipids provokes a clear decrease of the contribution of the 1654 cm^{-1} band in the helical region of the spectra, and of the 1630 cm^{-1} band, attributed to antiparallel sheets. On the other hand, the ~1660 cm^{-1} contribution, attributed to more "flexible" α helices, increased from 14% to 31%. A net increase in the 1680 cm^{-1} contribution was also observed. The latter could indicate that the secondary structure of the bound protein exhibits more beta turns [22] or shorter alpha helices [37].

It should be noted that both the blue shift of Trp fluorescence emission and the change in secondary structure occurred after binding either to PC or CL-containing vesicles, indicating similar conformational changes whatever the nature of the phospholipid polar head group.

6. Modification of lipid organisation by protein binding

A structural function of NDPK-D at the membrane level has been recently proposed [10], therefore a closer analysis of the NDPK-D-induced modifications at the membrane level is required. Fluorescence spectroscopy, and more specifically Laurdan polarity sensitivity, was first used. The GP parameter, which accounts for polar changes in the immediate vicinity of the probe, increased when CL- or PG-containing liposomes were in the presence of NDPK-D. This effect can be interpreted as a modification of this region organisation towards a more "rigid" state [17] in the presence of the protein in interaction with anionic polar head groups. Interestingly, despite the fact that NDPK-D interacts with zwitterionic membranes, it did not modify Laurdan fluorescence characteristics when incorporated into PC liposomes. This suggests that the interaction mechanism differs according to the charge of the membrane and that NDPK-D more easily modifies the polarity of Laurdan environment in a negatively charged membrane. Meanwhile, infrared measurements showed that binding of NDPK-D to both anionic and zwitterionic membranes triggers dehydration and loss of hydrogen bonding both at the level of phosphates and at the level of ester bonds (Figs. 4 and 5). Further investigation was conducted to determine the position of asymmetric and symmetric CH vibration bands and to illustrate the degree of ordering of the acyl chains in the bilayer. In the absence of NDPK-D, PC and PC–PE–CL liposomes presented CH_2 asymmetric and symmetric stretching bands at 2924 and 2853 cm^{-1}, respectively (Fig. 6). No significant spectral shifts were recorded after NDPK-D binding to PC liposomes. On the contrary, when NDPK-D was added to PC–PE–CL liposomes, a small but reproducible shift to higher wavenumbers was observed for both asymmetric and symmetric CH_2 bands. This shift of the acyl chain vibration band towards higher wavenumbers, which is in the same range as those previously reported in the literature for peptides or proteins interacting with lipid membranes [27,38–41] suggests a greater motional freedom of the CH_2 groups of lipids, and can be interpreted as an increase in acyl chain fluidity.

This result may seem to be in contrast with the effect illustrated by Laurdan experiments and GP measurements. On the one hand fluorescence experiments with Laurdan indicate that NDPK-D

induces a clear decrease in water content of the probe environment, which is generally associated with a decrease in membrane fluidity. On the other hand, FTIR data show a twofold effect of NDPK-D on the CL-containing membrane: a decrease in hydration at the polar head and ester bond level, together with an increase in the mobility of acyl chains. The first effect observed on FTIR spectra is in line with Laurdan experiments, as protein binding may chase water molecules from the polar region leading to dehydration and decrease in motility. The second effect on the acyl chains can be tentatively explained by protein splitting apart some lipid molecules and thus increasing the chain mobility. We suggest that this change takes place deeper in the lipid bilayer and is outside Laurdan direct environment. Indeed, Laurdan fluorescent moiety is located in the bilayer at the level of the glycerol backbone [42] and consequently is not suitable to monitor acyl chain modification.

To provide deeper insight into the forces that govern this interaction, we proposed a putative model for NDPK-D interaction with anionic or zwitterionic membranes (Fig. 9A and B respectively). As NDPK-D binding to liposomes results in dehydration of lipid head groups and as NaCl reduces the degree of binding, we can infer that a first step in the interaction is of electrostatic nature.

Three cationic residues (Arg89-Arg90-Lys91) are known to be involved in NDPK-D binding to CL [12]. The same residues may be involved in NDPK-D interaction with PC. Although globally neutral, PC presents a partial negative charge on the phosphate group. Some proteins or peptides were described in the literature to interact with this partial charge. For instance, melittin, an amphiphilic peptide of bee venom, is able to interact with PC membranes [43] inducing a conformational change at the phospholipid head group, characteristic of a response of PC head group to a positively charged surface.

Therefore, in what NDPK-D is concerned, positive charges on the "top" surface may be involved in the interaction both with PC and CL phosphate moiety. However, these charged residues are not the only ones involved in the interaction as the binding subsists in the presence of NaCl revealing another component which could be of hydrophobic nature. Proteins or parts of the proteins can insert into the membrane, thus chasing water molecules from the hydration layer of the ester bonds, and decreasing Laurdan polarity. This could correspond to a loop or to hydrophobic amino acids inserting into the membrane. A tempting hypothesis concerns the Trp residues. The maximum fluorescence emission wavelength shift, from 340 nm to 335–333 nm after protein binding to lipids, is in the same order of magnitude as that of peptides and proteins inserting into the membranes, (human dystrophin [30], LL-37 [31], amphibian antimicrobial peptide DD K [32], and melittin [33]), into a more hydrophobic environment [44]. We can draw a parallel with a study performed on secreted phospholipase A2 [45] which showed that this protein binds to PC membranes through a complex mixture of electrostatic and hydrophobic interactions and that one of the protein tryptophans (Trp 31) in essential for this interaction. Another example refers to melittin interacting with PC and PG in a 2-step mechanism, initial electrostatic, followed by re-orientation and/or insertion of peptide into hydrophobic membrane core [46].

Moreover, present data indicated that the mechanism that mediates the binding of NDPK-D depends of the nature of the phospholipid-containing membranes. In the case of CL, an increase in the acyl chain mobility, in addition to a dehydration effect, is observed which suggests that NDPK-D deeper penetrates into the CL than PC layer as already mentioned.

Brewster Angle Microscopy, performed on PC–PE–CL (2:1:1) monolayer used as a leaflet model system of the inner mitochondrial membrane, allowed us to monitor NDPK-D ability to disturb the phospholipid arrangement within the membrane. When injected under this monolayer, NDPK-D induced the formation of bright spots which, with time, increased in number but not in size. The average thickness of these spots was about 6.5 nm, the expected size of the NDPK-D hexamer (5 nm) bound to the monolayer (1.6 nm), thus confirming that we are dealing with lipid–protein complexes.

On a PC (Fig. 7B), PE or mixed PC–PE monolayer (not shown), and at similar surface pressure, no bright regions were observed. This would suggest that CL is mandatory for protein–lipid cluster formation. The clustering effect of NDPK-D on a pure CL monolayer was increased compared to that on PC–PE–CL, as the bright spots were more numerous and larger. Thus clustering can occur in the presence of protein and this phenomenon requires the presence of cardiolipin.

Such results may have important physiological consequences as, in view of CL roles in the mitochondrial membrane [47,48] a spatially defined distribution of this phospholipid is likely to affect metabolic processes but also mitochondrial dynamics and shape. A similar effect was reported on a system composed of CL and mitochondrial creatine kinase (mtCK). Previous studies showed that mtCK has a structural role, participating in the morphology of mitochondria [49]. Moreover, experiments performed with CL-containing monolayers or liposomes showed that this protein was able to induce segregation of CL [18,50,51]. Although mtCK and NDPK-D are phylogenetically distinct, they are both homo-oligomers exhibiting a second order symmetry with membrane-binding motifs exposed on both symmetrical faces [8,52]; they also have the capacity to anchor CL-containing membranes, to cross-link membranes and transfer lipids [12,13]. The tissue-specific expression level of NDPK-D and mtCK is inversely related, particularly in liver, where NDPK-D is highly expressed and mtCK is undetectable [10].

In this work, we have shown the ability of NDPK-D to affect the membrane fluidity (decreasing the hydration of esters and PO groups of the phospholipid membrane and increasing the acyl chain mobility) and cause the formation of CL clusters. This result reinforces the assumption that NDPK-D and mtCK could play similar roles in maintaining mitochondrial structure [10]. However, there are significant differences in their behaviour with respect to membrane binding. MtCK interaction with anionic membranes results in a decrease of the phospholipids acyl chain fluidity [52], whereas NDPK-D induced an increase of the acyl chain mobility. Contrary to mtCK, NDPK-D can interact with PC and its binding to anionic membranes is not sensitive to ionic strength. It should be noted that differences in the shape of liver (where NDPK-D is highly expressed) and heart mitochondria (where mtCK is abundant) have previously been described [53]. If both proteins are key factors in shaping mitochondria, then distinct behaviours of the two proteins might be one of the origins of the difference of mitochondrial shape observed between the liver and heart.

Acknowledgements

We are very grateful to Vincent Fitzpatrick for correcting the English, and to Dr. Marie-Lise Lacombe for helpful discussions and suggestions and for providing the plasmid for NDPK-D E.coli recombinant expression. We acknowledge funding from the University Lyon 1 and the CNRS.

References

[1] P.S. Steeg, G. Bevilacqua, R. Pozzatti, L.A. Liotta, M.E. Sobel, Altered expression of NM23, a gene associated with low tumor metastatic potential, during adenovirus 2 Ela inhibition of experimental metastasis, Cancer Res. 48 (1988) 6550–6554.
[2] V. Wallet, R. Mutzel, H. Troll, O. Barzu, B. Wurster, M. Veron, M.L. Lacombe, Dictyostelium nucleoside diphosphate kinase highly homologous to Nm23 and Awd proteins involved in mammalian tumor metastasis and Drosophila development, J. Natl. Cancer. Inst. 82 (1990) 1199–1202.
[3] I. Lascu, P. Gonin, The catalytic mechanism of nucleoside diphosphate kinases, J. Bioenerg. Biomembr. 32 (2000) 237–246.
[4] M. Boissan, S. Dabernat, E. Peuchant, U. Schlattner, I. Lascu, M.L. Lacombe, The mammalian Nm23/NDPK family: from metastasis control to cilia movement, Mol. Cell. Biochem. 329 (2009) 51–62.
[5] M.L. Lacombe, L. Milon, A. Munier, J.G. Mehus, D.O. Lambeth, The human Nm23/nucleoside diphosphate kinases, J. Bioenerg. Biomembr. 32 (2000) 247–258.

[6] D. Roymans, R. Willems, D.R. Van Blockstaele, H. Slegers, Nucleoside diphosphate kinase (NDPK/NM23) and the waltz with multiple partners: possible consequences in tumor metastasis, Clin. Exp. Metastasis 19 (2002) 465–476.
[7] M.F. Giraud, F. Georgescauld, I. Lascu, A. Dautant, Crystal structures of S120G mutant and wild type of human nucleoside diphosphate kinase A in complex with ADP, J. Bioenerg. Biomembr. 38 (2006) 261–264.
[8] L. Milon, P. Meyer, M. Chiadmi, A. Munier, M. Johansson, A. Karlsson, I. Lascu, J. Capeau, J. Janin, M.L. Lacombe, The human nm23-H4 gene product is a mitochondrial nucleoside diphosphate kinase, J. Biol. Chem. 275 (2000) 14264–14272.
[9] S. Morera, M.L. Lacombe, Y. Xu, G. LeBras, J. Janin, X-ray structure of human nucleoside diphosphate kinase B complexed with GDP at 2 A resolution, Structure 3 (1995) 1307–1314.
[10] M.L. Lacombe, M. Tokarska-Schlattner, R.F. Epand, M. Boissan, R.M. Epand, U. Schlattner, Interaction of NDPK-D with cardiolipin-containing membranes: structural basis and implications for mitochondrial physiology, Biochimie 91 (2009) 779–783.
[11] V. Adams, W. Bosch, J. Schlegel, T. Wallimann, D. Brdiczka, Further characterization of contact sites from mitochondria of different tissues: topology of peripheral kinases, Biochim. Biophys. Acta 981 (1989) 213–225.
[12] M. Tokarska-Schlattner, M. Boissan, A. Munier, C. Borot, C. Mailleau, O. Speer, U. Schlattner, M.L. Lacombe, The nucleoside diphosphate kinase D (NM23-H4) binds the inner mitochondrial membrane with high affinity to cardiolipin and couples nucleotide transfer with respiration, J. Biol. Chem. 283 (2008) 26198–26207.
[13] R.F. Epand, U. Schlattner, T. Wallimann, M.L. Lacombe, R.M. Epand, Novel lipid transfer property of two mitochondrial proteins that bridge the inner and outer membranes, Biophys. J. 92 (2007) 126–137.
[14] R.P. Agarwal, B. Robison, R.E. Parks Jr., Nucleoside diphosphokinase from human erythrocytes, Methods Enzymol. 51 (1978) 376–386.
[15] L.D. Mayer, M.J. Hope, P.R. Cullis, Vesicles of variable sizes produced by a rapid extrusion procedure, Biochim. Biophys. Acta 858 (1986) 161–168.
[16] R.C. MacDonald, R.I. MacDonald, B.P. Menco, K. Takeshita, N.K. Subbarao, L.R. Hu, Small-volume extrusion apparatus for preparation of large, unilamellar vesicles, Biochim. Biophys. Acta 1061 (1991) 297–303.
[17] T. Parasassi, G. De Stasio, G. Ravagnan, R.M. Rusch, E. Gratton, Quantitation of lipid phases in phospholipid vesicles by the generalized polarization of Laurdan fluorescence, Biophys. J. 60 (1991) 179–189.
[18] O. Maniti, M.F. Lecompte, O. Marcillat, B. Desbat, R. Buchet, C. Vial, T. Granjon, Mitochondrial creatine kinase binding to phospholipid monolayers induces cardiolipin segregation, Biophys. J. 96 (2009) 2428–2438.
[19] J. Saccani, S. Castano, B. Desbat, D. Blaudez, A phospholipid bilayer supported under a polymerized Langmuir film, Biophys. J. 85 (2003) 3781–3787.
[20] J. Voros, The density and refractive index of adsorbing protein layers, Biophys. J. 87 (2004) 553–561.
[21] P.K. Glasoe, F.A. Long, Use of glass electrodes to measure acidities in deuterium oxide, J. Physiol. Chem. 64 (1960) 188–190.
[22] A. Barth, Infrared spectroscopy of proteins, Biochim. Biophys. Acta 1767 (2007) 1073–1101.
[23] M. Jackson, H.H. Mantsch, The use and misuse of FTIR spectroscopy in the determination of protein structure, Crit. Rev. Biochem. Mol. Biol. 30 (1995) 95–120.
[24] W.K. Surewicz, H.H. Mantsch, D. Chapman, Determination of protein secondary structure by Fourier transform infrared spectroscopy: a critical assessment, Biochemistry 32 (1993) 389–394.
[25] J.L. Arrondo, F.M. Goni, J.M. Macarulla, Infrared spectroscopy of phosphatidylcholines in aqueous suspension. A study of the phosphate group vibrations, Biochim. Biophys. Acta 794 (1984) 165–168.
[26] R.N. Lewis, R.N. McElhaney, W. Pohle, H.H. Mantsch, Components of the carbonyl stretching band in the infrared spectra of hydrated 1,2-diacylglycerolipid bilayers: a reevaluation, Biophys. J. 67 (1994) 2367–2375.
[27] T. Granjon, M.J. Vacheron, C. Vial, R. Buchet, Mitochondrial creatine kinase binding to phospholipids decreases fluidity of membranes and promotes new lipid-induced beta structures as monitored by red edge excitation shift, laurdan fluorescence, and FTIR. Biochemistry 40 (2001) 6016–6026.
[28] D. Marsh, Lateral pressure in membranes, Biochim. Biophys. Acta 1286 (1996) 183–223.
[29] J. Hayer, M. Engel, M. Seifert, G. Seitz, C. Welter, Overexpression of nm23-H4 RNA in colorectal and renal tumours, Anticancer. Res. 21 (2001) 2821–2825.
[30] S. Legardinier, C. Raguenes-Nicol, C. Tascon, C. Rocher, S. Hardy, J.F. Hubert, E. Le Rumeur, Mapping of the lipid-binding and stability properties of the central rod domain of human dystrophin, J. Mol. Biol. 389 (2009) 546–558.
[31] R. Sood, Y. Domanov, M. Pietiainen, V.P. Kontinen, P.K. Kinnunen, Binding of LL-37 to model biomembranes: insight into target vs host cell recognition, Biochim. Biophys. Acta 1778 (2008) 983–996.
[32] R.M. Verly, M.A. Rodrigues, K.R. Daghastanli, A.M. Denadai, I.M. Cuccovia, C. Bloch Jr., F. Frezard, M.M. Santoro, D. Pilo-Veloso, M.P. Bemquerer, Effect of cholesterol on the interaction of the amphibian antimicrobial peptide DD K with liposomes, Peptides 29 (2008) 15–24.
[33] H. Raghuraman, A. Chattopadhyay, Interaction of melittin with membrane cholesterol: a fluorescence approach, Biophys. J. 87 (2004) 2419–2432.
[34] S.A. Tatulian, R.L. Biltonen, L.K. Tamm, Structural changes in a secretory phospholipase A2 induced by membrane binding: a clue to interfacial activation? J. Mol. Biol. 268 (1997) 809–815.
[35] J. Cladera, M. Sabes, E. Padros, Fourier transform infrared analysis of bacteriorhodopsin secondary structure, Biochemistry 31 (1992) 12363–12368.
[36] T. Granjon, O. Maniti, Y. Auchli, P. Dahinden, R. Buchet, O. Marcillat, P. Dimroth, Structure–function relations in oxaloacetate decarboxylase complex. Fluorescence and infrared approaches to monitor oxomalonate and Na(+) binding effect, PLoS One 5 (2010) e10935.
[37] N.A. Nevskaya, Y.N. Chirgadze, Infrared spectra and resonance interactions of amide-I and II vibration of alpha-helix, Biopolymers 15 (1976) 637–648.
[38] E. Dufour, M. Subirade, F. Loupil, A. Riaublanc, Whey proteins modify the phase transition of milk fat globule phospholipids, Lait 79 (1999) 217–228.
[39] A. Gericke, E.R. Smith, D.J. Moore, R. Mendelsohn, J. Storch, Adipocyte fatty acid-binding protein: interaction with phospholipid membranes and thermal stability studied by FTIR spectroscopy, Biochemistry 36 (1997) 8311–8317.
[40] O. Maniti, I. Alves, G. Trugnan, J. Ayala-Sanmartin, Distinct behaviour of the homeodomain derived cell penetrating peptide penetratin in interaction with different phospholipids, PLoS One 5 (2010) e15819.
[41] Y.P. Zhang, R.N. Lewis, R.S. Hodges, R.N. McElhaney, Interaction of a peptide model of a hydrophobic transmembrane alpha-helical segment of a membrane protein with phosphatidylcholine bilayers: differential scanning calorimetric and FTIR spectroscopic studies, Biochemistry 31 (1992) 11579–11588.
[42] P.L. Chong, P.T. Wong, Interactions of Laurdan with phosphatidylcholine liposomes: a high pressure FTIR study, Biochim. Biophys. Acta 1149 (1993) 260–266.
[43] E. Kuchinka, J. Seelig, Interaction of melittin with phosphatidylcholine membranes. Binding isotherm and lipid head-group conformation, Biochemistry 28 (1989) 4216–4221.
[44] A.S. Ladokhin, P.W. Holloway, Fluorescence of membrane-bound tryptophan octyl ester: a model for studying intrinsic fluorescence of protein–membrane interactions, Biophys. J. 69 (1995) 506–517.
[45] S.K. Han, K.P. Kim, R. Koduri, L. Bittova, N.M. Munoz, A.R. Leff, D.C. Wilton, M.H. Gelb, W. Cho, Roles of Trp31 in high membrane binding and proinflammatory activity of human group V phospholipase A2, J. Biol. Chem. 274 (1999) 11881–11888.
[46] T.H. Lee, H. Mozsolits, M.I. Aguilar, Measurement of the affinity of melittin for zwitterionic and anionic membranes using immobilized lipid biosensors, J. Pept. Res. 58 (2001) 464–476.
[47] U. Schlattner, M. Tokarska-Schlattner, S. Ramirez, A. Bruckner, L. Kay, C. Polge, R.F. Epand, R.M. Lee, M.L. Lacombe, R.M. Epand, Mitochondrial kinases and their molecular interaction with cardiolipin, Biochim. Biophys. Acta 1788 (2009) 2032–2047.
[48] Z.T. Schug, E. Gottlieb, Cardiolipin acts as a mitochondrial signalling platform to launch apoptosis, Biochim. Biophys. Acta 1788 (2009) 2022–2031.
[49] H. Lenz, M. Schmidt, V. Welge, T. Kueper, U. Schlattner, T. Wallimann, H.P. Elsasser, K.P. Wittern, H. Wenck, F. Staeb, T. Blatt, Inhibition of cytosolic and mitochondrial creatine kinase by siRNA in HaCaT- and HeLaS3-cells affects cell viability and mitochondrial morphology, Mol. Cell. Biochem. 306 (2007) 153–162.
[50] O. Maniti, M. Cheniour, M.F. Lecompte, O. Marcillat, R. Buchet, C. Vial, T. Granjon, Acyl chain composition determines cardiolipin clustering induced by mitochondrial creatine kinase binding to monolayers, Biochim. Biophys. Acta 1808 (2011) 1129–1139.
[51] R.F. Epand, M. Tokarska-Schlattner, U. Schlattner, T. Wallimann, R.M. Epand, Cardiolipin clusters and membrane domain formation induced by mitochondrial proteins, J. Mol. Biol. 365 (2007) 968–980.
[52] K. Fritz-Wolf, T. Schnyder, T. Wallimann, W. Kabsch, Structure of mitochondrial creatine kinase, Nature 381 (1996) 341–345.
[53] F. Forner, L.J. Foster, S. Campanaro, G. Valle, M. Mann, Quantitative proteomic comparison of rat mitochondria from muscle, heart, and liver, Mol. Cell. Proteomics 5 (2006) 608–619.